4 Visualization

4.1 Ignition Diagnostics based on Spark-Induced Breakdown Spectroscopy for Gas-Engine Applications

Laura Merotto, Thomas Kammermann, Davide Bleiner, Patrik Soltic

Abstract

Spark ignition engines involve cyclic variation of the combustion process. A better understanding of the underlying mechanisms driving these variations is of major importance for the optimization in terms of emissions and fuel economy. The location and growth rate of the initial flame kernel is one of the factors affecting the magnitude and timing of the peak cylinder pressure. In turns, the rate of development of the initial flame kernel is mainly affected by the local fuel concentration and homogeneity near the spark gap and the local flow conditions, such as turbulent structure and magnitude. Currently, natural gas-dedicated engines with direct injection combustion concepts are being developed to improve the thermal efficiency and take advantage of the lower CO_2 emissions compared to gasoline and diesel. The higher knock resistance of methane allows increasing the compression ratio, but this also makes it a more challenging environment to successfully initiate combustion, especially in lean or stratified combustion or at high EGR conditions. This leads to higher requirements on the ignition system and on the control of the mixture formation process.
A diagnostic tool for providing information on the mixture composition at the spark plug during spark timing is highly valuable for research and development purposes. Spark-Induced Breakdown Spectroscopy (SIBS) is a measurement technique in which the plasma formed by spark generation between two electrodes is used as the excitation source for optical emission spectroscopy. The light emission from the species excited by the plasma is related to the local mixture conditions, and therefore can be used as a diagnostic tool to deliver information on local conditions around the spark plug during the ignition attempt. In SI engines, SIBS can be used in the combustion chamber with minor engine modifications and is therefore a promising alternative to other investigation techniques, as Laser-Induced Breakdown Spectroscopy (LIBS), where a laser has to be coupled to the combustion chamber.
In this work, different quiescent mixture compositions at ambient temperature and elevated pressure conditions were investigated in a constant volume cell. A spectrometer and an intensified camera were used to capture the plasma emission from the electrical discharge in order to develop a SIBS-based measurement technique for ignition events investigation.
The role of methane, air and hydrogen on the electrical discharge characteristics and the plasma emissions were investigated. Moreover, atomic and molecular spectral emissions in different ambient conditions and for different mixtures were analyzed and compared, with the aim to obtain a deeper insight on the SIBS response to the complex

physical and chemical phenomena underlying the ignition event. Results show that the proposed technique is a compact and versatile tool for applications involving atomic and molecular species detection in different ambient conditions.

Kurzfassung

Ottomotoren unterliegen zyklischen Variationen im Verbrennungsprozess. Ein vertieftes Verständnis der zugrunde liegenden Mechanismen, welche diese zyklischen Schwankungen antreiben, ist fundamental in Bezug auf die Optimierung von Emissionen und Kraftstoffverbrauch. Der Ort des Flammenkerns und dessen Wachstumsrate sind wichtige Faktoren, welche die Amplitude und den Zeitpunkt des maximalen Zylinderdrucks beeinflussen. Die Entwicklungsgeschwindigkeit des anfänglichen Flammenkerns wird wiederum hauptsächlich durch die lokale Brennstoffkonzentration und -homogenität in der Nähe der Funkenstrecke und die lokalen Strömungsbedingungen, wie turbulente Struktur und Größe, beeinflusst. Gegenwärtig werden Motoren für magere Gemische und für direkteinspritzende Verbrennungskonzepte entwickelt, um den thermischen Wirkungsgrad zu verbessern und die, im Vergleich zu Benzin und Diesel, geringeren CO_2-Emissionen zu nutzen. Die höhere Klopffestigkeit von Methan erlaubt es, das Kompressionsverhältnis zu erhöhen. Dies führt jedoch auch zu erschwerten Bedingungen um eine Verbrennung erfolgreich einzuleiten, insbesondere im Mager- und Schichtladungsbetrieb sowie bei hohen Abgasrückführraten. All diese Faktoren erhöhen die Anforderungen an das Zündsystem und an die Steuerung des Gemischbildungsprozesses.
Ein Diagnosewerkzeug zum Bereitstellen von Informationen über die Gemischzusammensetzung an der Zündkerze während des Zündzeitpunkts ist sehr wertvoll. Funkeninduzierte Plasmaspektroskopie ist eine Technik, bei der das durch Funkenbildung zwischen zwei Elektroden gebildete Plasma als Anregungsquelle für die optische Emissionsspektroskopie verwendet wird. Die Lichtemission der durch das Plasma angeregten Spezies hängt vom lokalen Gemisch ab und kann daher als ein Diagnosewerkzeug verwendet werden, um während des Zündversuchs Informationen über örtliche Bedingungen um die Zündkerze zu liefern. In Ottomotoren kann diese Methodik mit minimalen Motormodifikationen in der Brennkammer eingesetzt werden und ist daher eine vielversprechende Alternative zu anderen Untersuchungstechniken wie laserinduzierte Plasmaspektroskopie, bei welcher ein Laser in den Brennraum gekoppelt werden muss.
In dieser Arbeit wurden verschiedene ruhende Gemischzusammensetzungen bei Umgebungstemperatur und erhöhten Druckbedingungen in einer Konstantvolumenzelle untersucht. Ein Spektrometer und eine intensivierte Kamera wurden verwendet um die Plasmaemission der elektrischen Entladung zu erfassen, um eine SIBS-basierte Messtechnik für die Untersuchung von Zündereignissen zu entwickeln.
Die Rolle von Methan, Luft und Wasserstoff auf die elektrischen Entladungseigenschaften und die Plasmaemissionen wurden untersucht. Darüber hinaus wurden atomare und molekulare Spektralemissionen unter verschiedenen Umgebungsbedingungen und für verschiedene Gemische analysiert und verglichen, um ein besseres Verständnis der Spektren der komplexen physikalischen und chemischen Phänomene zu erlangen, die dem Zündvorgang zugrunde liegen. Die Ergebnisse zeigen, dass die erarbeitete Methodik ein kompaktes und vielseitiges Werkzeug für Anwendungen ist, bei denen atomare und molekulare Spezies unter verschiedenen Umgebungsbedingungen detektiert werden.

1 Introduction

The combustion process in spark ignition engines involves cyclic variation of combustion, thus resulting in difficult optimization in terms of engine emissions and fuel economy since, for example, fast burning cycles are critical for knock and slow burning cycles deteriorate efficiency. Several investigations have been performed in the last decades with the aim to overcome these difficulties.

Lean-burn spark-ignition (SI) engines have been developed to improve fuel economy and reduce emissions [1–3]. Although lean operation has proven to result in such important advantages [4], mixture air to fuel (A/F) ratio increase results in more prominent cycle-by-cycle variations in flame development, limiting the lean-burn operation range. Therefore, aim of research in this framework is to achieve the understanding needed to ensure an extension of the current limits of A/F ratio for engine operation. In order to do so, the investigation of local mixture conditions around the spark plug is of major importance, since they determine the successfulness of the ignition attempt, and in turn affect the initial flame growth and the establishment of turbulent combustion.

As an alternative to homogeneous mixtures as they are typically achieved with port-fuel injection direct injection enable charge stratification [5,6], i.e. the fuel/air mixture can be fuel-richer around the spark plug. Previous research show [7] that the growth rate and location of the initial flame kernel is one of the major factors affecting the magnitude and timing of the peak cylinder pressure. Several studies [8,9] show that the ignition limits in terms of air to fuel ratio are strongly affected by the presence of turbulence in the flow. In turns, the rate of development of the initial flame kernel is affected by the local fuel concentration near the spark gap [2]. Therefore, a need for better understanding and control of such a concentration arises.

Currently, natural gas-dedicated engines with stoichiometric or lean-burn combustion concepts are being developed to improve the thermal efficiency and take advantage of the lower CO_2 emissions compared to gasoline and diesel. The higher knock resistance of methane allows increasing the compression ratio compared to today's bivalent engines found in the passenger car sector. But this also affects the demands on an ignition system due to higher pressures at spark timing, resulting in an increased demand on the insulation resistance on the coil and spark plug. This makes it a more challenging environment to successfully initiate combustion. Recent developments in gas engines include direct injection strategies. Reynolds et. al. [10] have investigated a direct-injection lean-burn natural gas engine. Their results show that better fuel consumption is obtained at higher air to fuel ratios when a stratified charge is used. In [11] the effect of different injection strategies for methane, hydrogen and hydrogen-enriched methane in a spark ignition engine are investigated. The authors show that direct injection direction and timing affect mainly the early phase of combustion, whereas the later combustion phase is mainly influenced by the global stoichiometry and the fuel composition. It is important to notice that air to fuel ratio measurements are of great importance in such engines, because within charge stratification, fuel concentration is higher close to the spark plug, thus resulting in higher flames temperature and higher NO_x emissions [11]. Other concepts, like systems with actively fueled prechambers, have also gained on attention [12]. In such concepts, where the stoichiometry within the prechamber can differ significantly from the stoichiometry of the main combustion chamber, non-intrusive optical measurement fuel concentration measurement techniques are the only option for stoichiometry diagnostics in the prechamber.

Various approaches have been used by several researchers to measure the air to fuel ratio or fuel concentration in SI engines, including Laser induced breakdown Spectroscopy (LIBS). LIBS is a well established measurement technique in the research community [13,14], and the laser pulse can be successfully used as a diagnostic tool for a variety of applications, including engines. Ferioli and Buckley[15] demonstrated the possibility to obtain quantitative air/fuel equivalence ratios for methane and propane in air. The applicability of LIBS in a single cylinder engine using the ratios of the H_α/O_{777}, the H_α/N_{746} and $H_\alpha/N_{742\text{-}746}$ emission lines were tested, showing good results and suggesting this method for in-cylinder, cycle resolved air-fuel ratio measurements [16]. Phuoc and White [17] discussed simultaneous laser ignition and equivalence ratio measurement using laser-induced gas breakdown in methane–air and hydrogen/air mixtures using H_α (656 nm) and the O triplet near 777 nm. Rahman and Kawahara [18] measured the equivalence ratio using LIBS and discussed the accuracy of spatially, temporally, and spectrally resolved measurements. However, it is difficult to apply a LIBS system to equivalence ratio measurements around a spark plug due to the difficulty with laser access in a practical SI engine [19].

Spark-induced breakdown spectroscopy (SIBS), a measurement technique in which the source of excitation is the energy delivered by an electric spark discharge, is a feasible alternative to laser spectroscopy methods in SI engines, and can be used in a combustion chamber with no engine modifications, except an optical access. In this technique, the signal detection and spectroscopy is similar to LIBS; however, spark generation occurs between two electrodes, and the spark itself is used as the light source to obtain information on the mixture concentration through spectral analysis of the light emitted by the excited species. Spark-induced breakdown spectroscopy can be used as a diagnostic tool to characterize the local mixture conditions around the spark plug during the ignition attempt.

From SIBS spectral response, the local fuel-air equivalence ratio of different fuels such as methane [7,20], hydrogen [18], propane and isooctane [21] can be derived or plasma temperatures [22] determined. Ando and Kuwahara [23] and Fansler et al. [21] reported measurements of the equivalence ratio at the spark gap using the ratio of CN (388 nm) and OH (306 nm) emission intensity from the spark. They determined the cycle-resolved local fuel/air ratio in the spark gap, and evaluated the utility of SIBS as an engine diagnostic tool. However, they reported that it is difficult to detect the equivalence ratio under lean mixture conditions due to lack of the linearity of CN/OH emission intensity ratio. In [18], the authors sought to characterize the effects of ambient pressure at ignition timing on spectral line emissions and to improve the accuracy of SIBS measurements by taking into account the pressure dependency of atomic emissions. Spectrally resolved emission spectra of plasma generated by a spark plug were measured through an optical fiber housed in the center electrode of the spark plug. A calibration map representing the correlation of air excess ratio (air/fuel) with both intensity ratio and pressure at ignition timing was created by taking into account the effect of the corresponding pressure at ignition on spectral line intensity. The calibration line and calibration map were subsequently used for quantitative measurements of the local air excess ratio for both port injection and direct injection strategies to investigate the effects of the corresponding pressure at ignition timing on the accuracy of SIBS measurements.

Kawahara [20] also determined the local equivalence ratio of a methane/air mixture in a laminar premixed flame using SIBS with a fiber-coupled intensified charge coupled device (ICCD) spectrometer. The emission intensities of OH, CN, and NH spectra

under several equivalence ratio conditions were measured and discussed as a way to measure the equivalence ratio using the intensity ratios of CN/OH and CN/NH. In this investigation, the intensity ratio of the H_α/O atomic emission lines is used to measure the equivalence ratio of a premixed mixture and compared with the applicability of the intensity ratios of CN/OH and CN/NH. However, their results showed that the H_α/O intensity ratio is more suited for measuring the equivalence ratio than CN/NH under lean mixture condition, thus suggesting that further investigation is needed in order to better understand the ongoing processes and to further improve SIBS technique reliability and versatility.

With this aim, SIBS as a diagnostic tool for methane/air and hydrogen enriched methane mixtures in engine relevant conditions was spatially and temporally investigated at Empa [24]. In this work, the spectral signal dependency on air/fuel equivalence ratio as well as on methane substitution by hydrogen was investigated focusing on spectral emissions of OH, NH and CN. Spatially resolved measurements provided insight in the molecular emissions distributions along the spark gap. Results showed that although a dependence of the intensity ratios of CN_{388}/OH_{306} and CN_{388}/NH_{336} on the fuel-air ratio was found, shot to shot repeatability was high, thus suggesting further investigation on the atomic emission lines in order to further improve the technique.

The present work presents the SIBS-based diagnostic tool developed at Empa for ignition diagnostics for engine applications. The technique shows a high versatility, allowing investigation of different quiescent mixture compositions at ambient temperature and elevated pressure conditions using a small constant volume cell. A spectrometer and an intensified camera are used to capture the plasma emission from the electrical discharge, and spectral emissions are analyzed in order to gather information on the local mixture composition around the spark plug. Spectral emissions in different ambient conditions and for different mixtures are compared and discussed, with the aim to obtain a deeper insight on the SIBS response to the complex physical and chemical phenomena underlying the ignition event. First, different single gases' emissions are discussed; then, the spectral response from two components blends is taken into account, discussing the different results obtained from inert and reactive mixtures. Atomic and molecular emissions are considered and compared.

Results show that the proposed technique is a compact and versatile tool for applications involving atomic and molecular species detection in different ambient conditions. A fiber-optic equipped spark plug is then presented, which is the first step in running engine application of the proposed SIBS-based diagnostics.

2 Methods

2.1. Experimental setup

The experimental setup used for the present work was developed for spectral and temporally resolved measurements, and is shown in Figure 1. A detailed description of the setup can be found in [24].

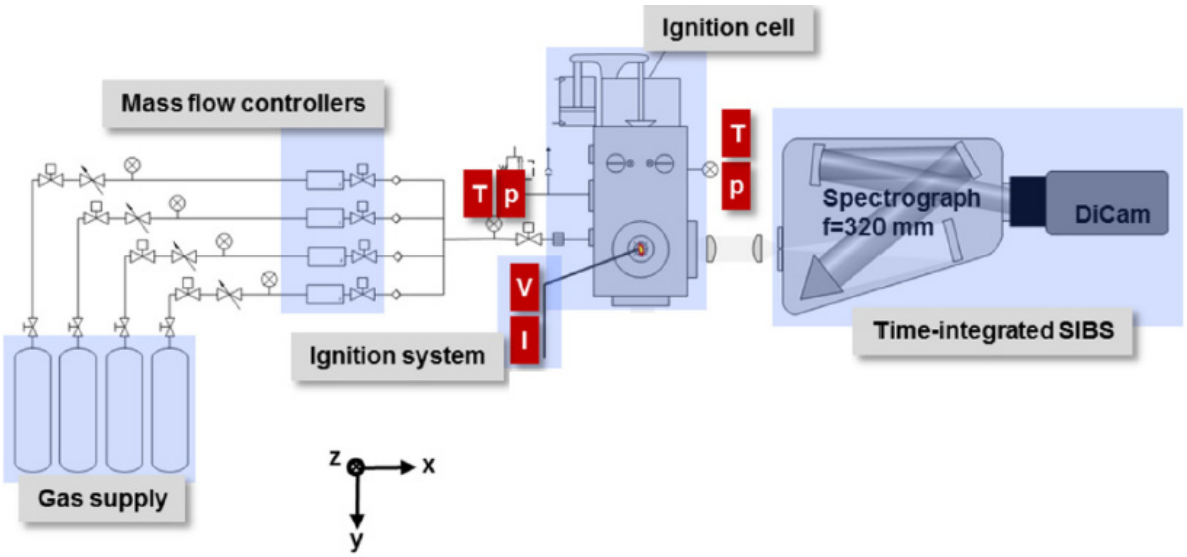

Figure 1: Sketch of the experimental setup for SIBS-based ignition diagnostics.

A small constant volume ignition cell, designed for optical investigation of emissions from sparks in homogeneous quiescent mixtures and coupled with a spectrometer was used. The cell is equipped with pneumatically actuated in- and outlet-valves, an absolute pressure sensor (Keller PAA-33X) for the control of the filling process and with a piezoelectric pressure transducer (Kistler 6052C) to measure the transient in-cell pressure. Gas supply was controlled via mass flow controllers (Bronkhorst).
The ignition system was based on a commercially available ignition coil (BERU), providing 60 mJ of secondary energy with a maximum spark duration of 2.2 ms at 800 V zener load. The coil was mounted on a commercially available M10 thread spark plug (NGK DIMR8A10) with double fine wire electrodes. The electrode gap was 1 mm. Current and voltage signals are captured via a data acquisition card (National Instruments PXI-5105, 60 MHz) or via an oscilloscope with 1 GHz bandwidth (LeCroy Wavesurfer 10).
The light emitted by the spark plasma was collected via a lens system through sapphire windows and transferred to the spectrometer slit. A slit width of 50 µm has been used throughout this study. Wavelength calibration spectra have been captured from a mercury neon lamp. A grating of 150 mm^{-1} was used on the Princeton Instruments spectrograph (Acton IsoPlane SCT 320) with a focal length of 320 mm. An intensified CCD camera (PCO DiCam Pro) with a detector size of 1280×160 pixels was used to collect the spectra, with a resulting spectral resolution of 1.7 nm for the 150mm^{-1} grating.
A custom made trigger box was used to trigger the intensified CCD camera after the breakdown phase, using the secondary current as trigger input. The output signal of the comparator has an intrinsic delay of 50 ns, but allows overcoming the jitter with respect to the ignition timing of the coil ignition system. This ensures that the chosen gate timing with respect to the breakdown (time = 0) remains the same within a measurement series.

2.2. Electrical discharge structure and triggering strategy

The information that can be obtained analyzing spectral emissions strongly depend on the triggering strategy, i.e. on the time range selected for acquiring the optical measurements. It is well known [8] that the electrical discharge occurring between the spark plug electrodes can be divided into three phases (breakdown, arc and glow discharge), characterized by different time scales.

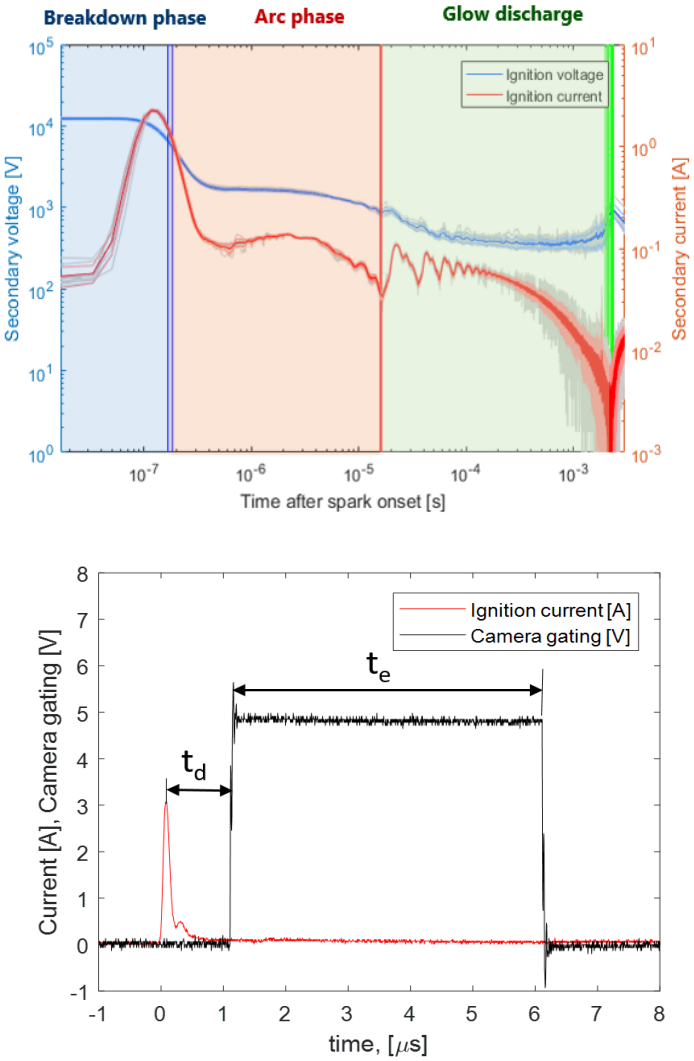

Figure 2: Top: Electrical discharge structure. Depending on the triggering strategy selected, it is possible to focus the measurement in the breakdown phase, in the arc phase or in the glow phase. Bottom: illustration of camera exposure time (t_e) and triggering delay (t_d).

The physical phenomena underlying the electrical discharge structure have a major impact on the spectral emissions features, and therefore on the information obtainable from this kind of analysis. Namely, breakdown occurrence causes the gas molecules in the ignition area to break into atoms and ions. Molecular recombination starts after some hundreds nanoseconds [8] from breakdown, thus leading to significantly different spectral emissions. Consequently, if measurements are triggered closer to the time at which breakdown occurs, atomic lines will appear in the spectral emission, while

molecular emissions will be revealed some microseconds or milliseconds after breakdown.
The general structure of an electrical discharge is sketched in the left part of Figure 2, while the right part shows a typical secondary current signal and the camera gating time. The exposure time (t_e) is the time interval during which a spectral emission is acquired. The time delay (t_d) between the secondary current spike due to breakdown occurrence and the onset of the camera gating is also indicated, and will be referred to as "delay" in the following sections.
Both the exposure time and the delay affect the spectral emissions' features, as discussed in the following section.

3. Results and discussion

3.1. Single gases emissions: effect of exposure time and delay

As mentioned in the previous section, different emissions can be measured depending on the gating strategy selected. In order to select a gating strategy for the gases investigated in this work, preliminary tests were performed varying the exposure and the delay with the aim to optimize the signal to noise ratio. Results showed that the better signal to noise ratio is obtained when the spectra acquisition is gated right after the breakdown occurs.
An example of emission spectra is given in Figure 3 for 5 µs exposure time and in Figure 4 for 2 ms exposure time. The spectra recorded using four different pure gases (air, hydrogen, nitrogen and methane) are shown, together with an indication of the main emission lines recognizable.

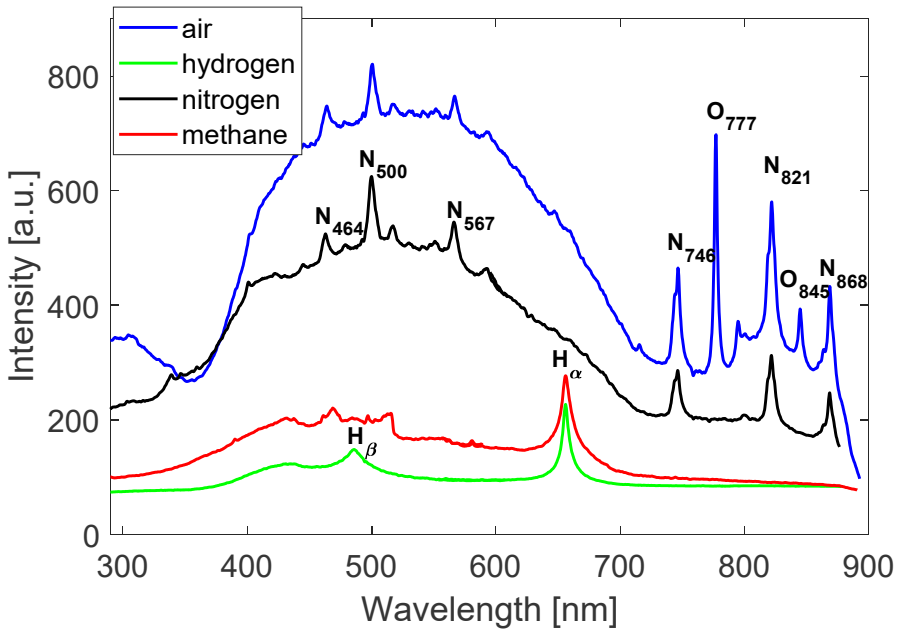

Figure 3: Spectral emissions for pure gases (air, hydrogen, nitrogen and methane) at 10 bar absolute pressure. Exposure time t_e = 5 µs, delay t_d = 0.

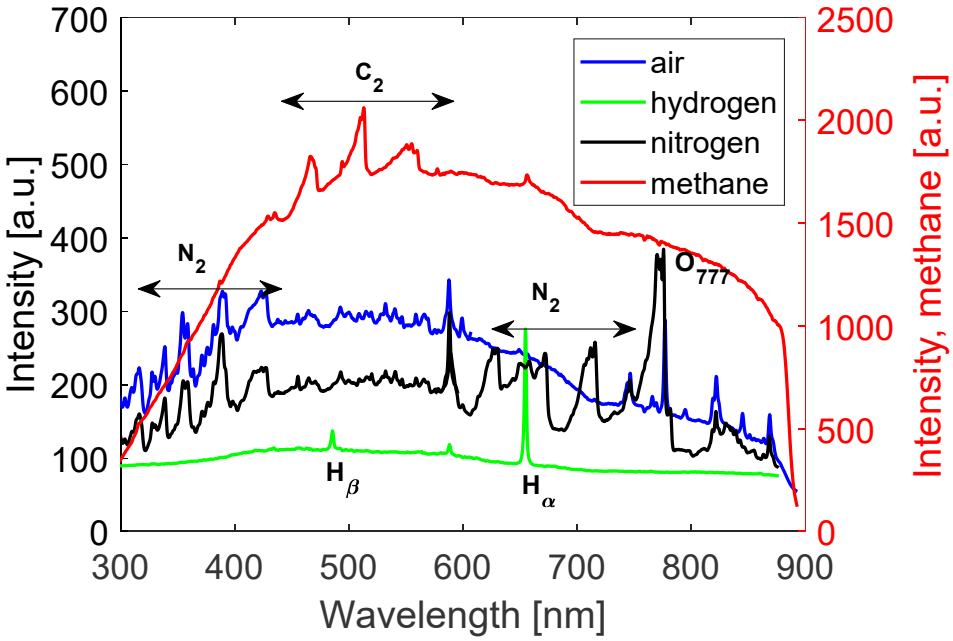

Figure 4: Spectral emissions for pure gases (air, hydrogen, nitrogen and methane) at 10 bar absolute pressure. Exposure time t_e = 2 ms, delay t_d = 0. Due to high continuum emission, methane spectral signature is plotted on a secondary axis (right, red axis).

The exposure time is not the only gating parameter affecting the measurements features: delay also plays a major role, as can be seen from the spectra plotted in Figure 5, in which emissions obtained from pure air at different delays are plotted. Tests were performed at 10 bar ambient pressure, and the exposure time is 100 ns.

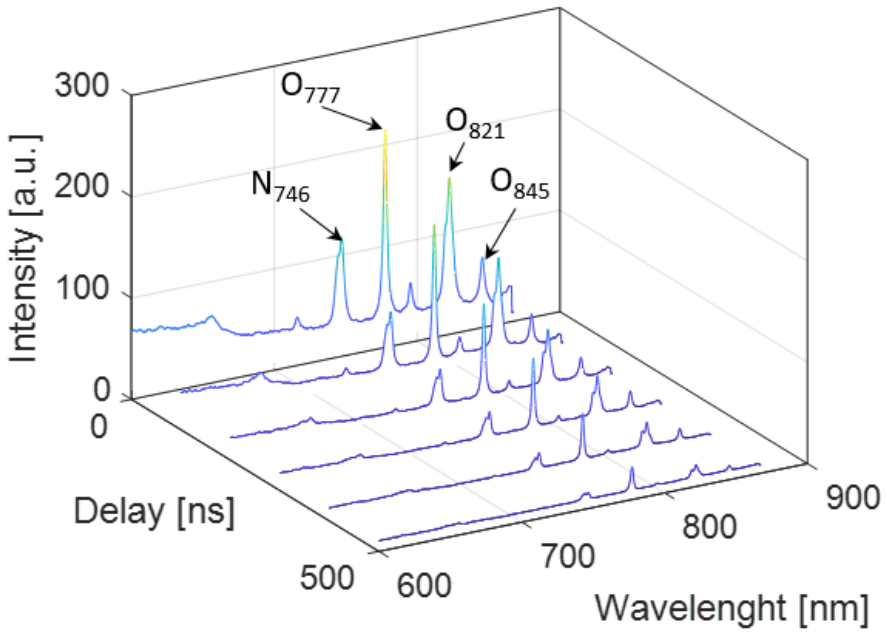

Figure 5: Spectral emissions obtained for air at different delay times. The camera exposure is 100 ns, and absolute pressure is 10 bar.

It can be noticed from Figure 5 that both the continuum emission and the atomic lines measured steadily decrease with time. In particular, the emission intensities from nitrogen at 746 nm and from oxygen at 777 nm decrease towards a minimum value, and they can be clearly recognized up to a delay value of approximately 1 μs, as shown in Figure 6. The atomic peaks ratios follow a different trend (Figure 7), being around 0.5 immediately after breakdown, and approaching a value of approximately 1 as the delay increases towards 1000 ns. It can therefore be concluded that the choice of delay and gating times is of major importance for correlations of peak intensity ratios with other parameters.

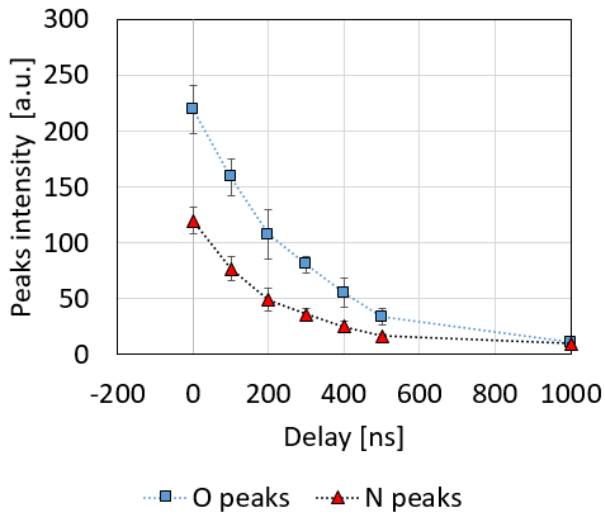

Figure 6: Oxygen (777 nm) and Nitrogen (746 nm) peaks intensity vs. delay time. Pure air, p = 10 bar.

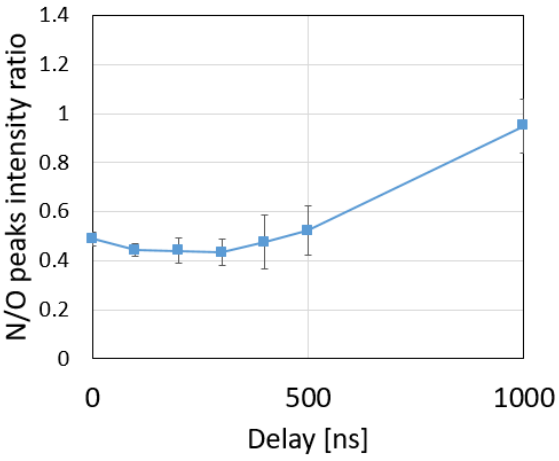

Figure 7: Nitrogen (746 nm) and Oxygen (777 nm) peaks intensity ratio vs. delay time. Pure air, p = 10 bar.

Based on the results reported for air, and based on similar results (not reported here) for other gases or mixtures, it was possible to estimate the time range after breakdown in which the emissions of interest are visible, and thus to select the most appropriate gating strategy for each case, as reported in the following sections.

3.2. Methane/hydrogen mixtures: non-reactive cases

The effect of hydrogen addition to methane was investigated, by measuring the spectral emissions of mixtures having hydrogen volume percentage ranging from 0 to 100%. Tests were performed at 2 bar, with exposure time of 300 μs. The obtained results are shown in Figure 8. The exposure time is long enough for the C_2 Swan bands to clearly appear in the spectra, between 468 and 557 nm. With increasing hydrogen content, these peaks intensity steadily decrease, while the hydrogen Balmer-α line increases. When 100% hydrogen is used, also the Balmer-β line becomes prominent enough to be clearly recognized at 486 nm.

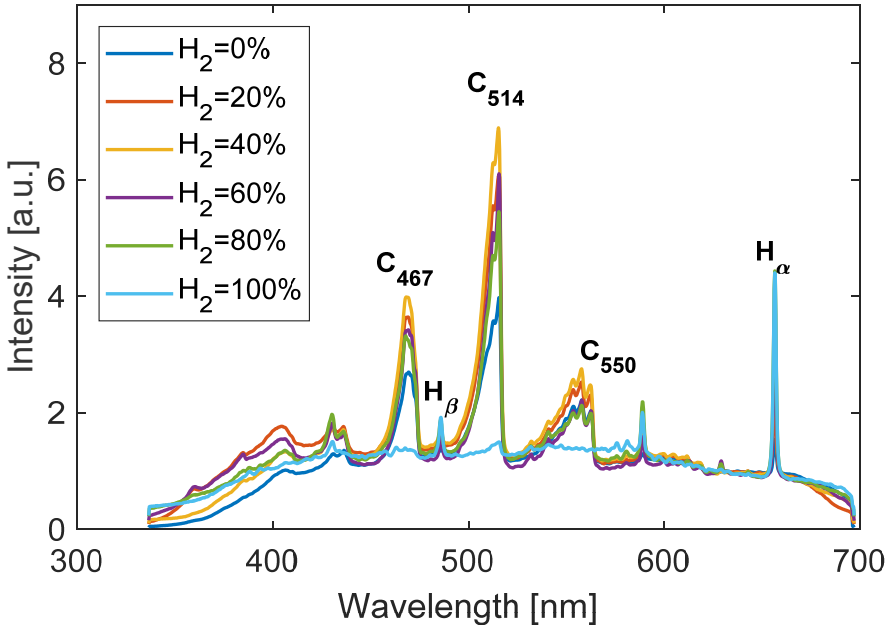

Figure 8: Spectral emissions for methane/hydrogen mixture with different volumetric hydrogen content. Absolute pressure 2 bar, exposure time t_e = 300 µs.

In order to quantify the peaks intensity variation with hydrogen addition, the peaks of hydrogen (H_α) at 656 nm and the peaks of the Swan bands at 514 (C_{514}) and 550 (C_{550}) were considered. The H/C peak intensity ratios vs. hydrogen content are plotted in Figure 9. Considering H_α/C_{514} it can be noticed that the ratio varies only slightly (0.4-0.5) up to a hydrogen content of approximately 60%. With further increase, the H/C increase becomes steeper, changing from 0.8 for 80% H_2 to 4.8 for 100% H_2. A similar behavior is obtained with H_α/C_{550}, with peaks intensity ratio increasing from about 1 to 4.7.

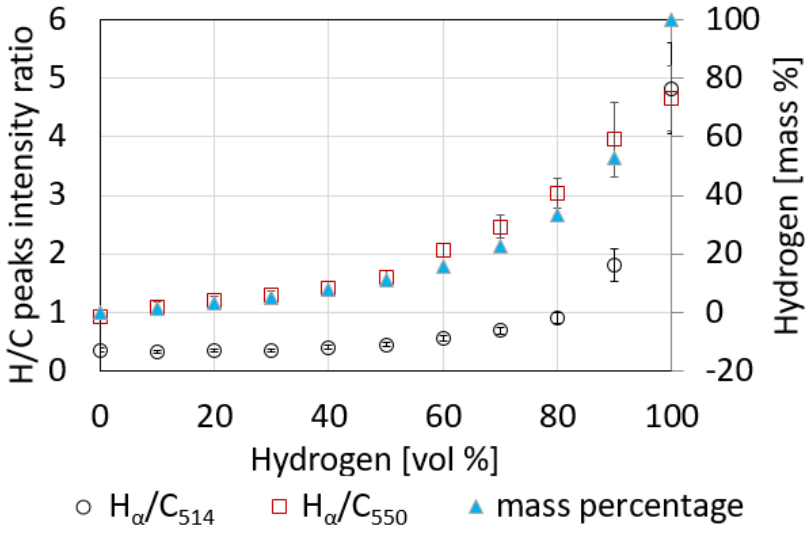

Figure 9: H/C ratio variation vs. hydrogen content in methane, for the mixtures containing different hydrogen percentages. The hydrogen mass percentage corresponding to the volume percentage is also shown (right y-axis).

This trend can be explained taking into account the mass percentage variation with respect to the volume percentage variation. Namely, the H/C intensity ratios follow the same trend as the hydrogen mass percentage (also shown in Figure 9), thus showing that the spectral emissions can be used as a diagnostic tool also in the methane/hydrogen case.

3.3. Methane/air mixtures: reactive cases

Molecular and atomic emissions for a methane/air mixture at stoichiometric conditions (λ = 1) were investigated, and the spectral emissions were compared to the spectra obtained for the corresponding pure gases. Tests were performed at 10 bar, the delay with respect to breakdown was set to 0, and the exposure times were 2 ms for molecular emissions measurements and 5 µs for atomic emission measurements. Results are shown in Figure 10 and Figure 11. When the results for the mixture are compared to the results obtained for the single gases at the same conditions, it can be seen that the overall spectral emission change significantly depending on the exposure time.
At long exposure times (2 ms, Figure 10), the spectral signature for methane/air mixture does not show the same features as the corresponding pure gases. In particular, the carbon Swan bands for C_2 which appear in the pure methane spectral emissions disappear with the presence of oxygen and nitrogen.

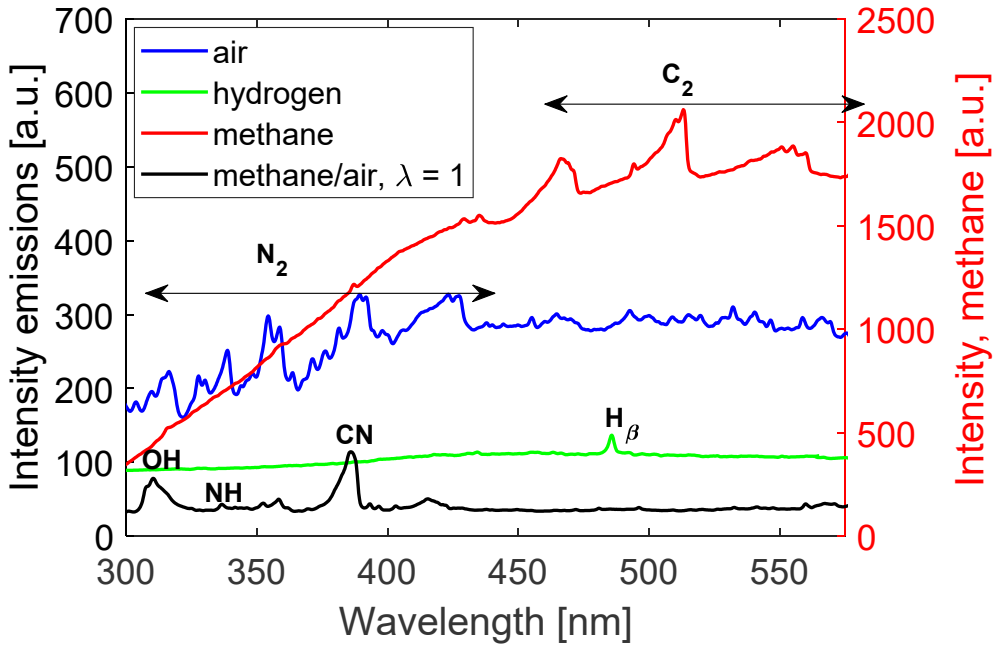

Figure 10: Spectral emissions for pure gases and for methane/air mixture, at 2 ms exposure time, absolute pressure 10 bar.

Shortly after breakdown (exposure 5 µs, Figure 11), the atomic emission of hydrogen at 656 nm, nitrogen at 746 nm and oxygen at 777 nm can be clearly recognized. The same atomic lines are recognizable when the spectral emissions of the corresponding pure gases are examined.

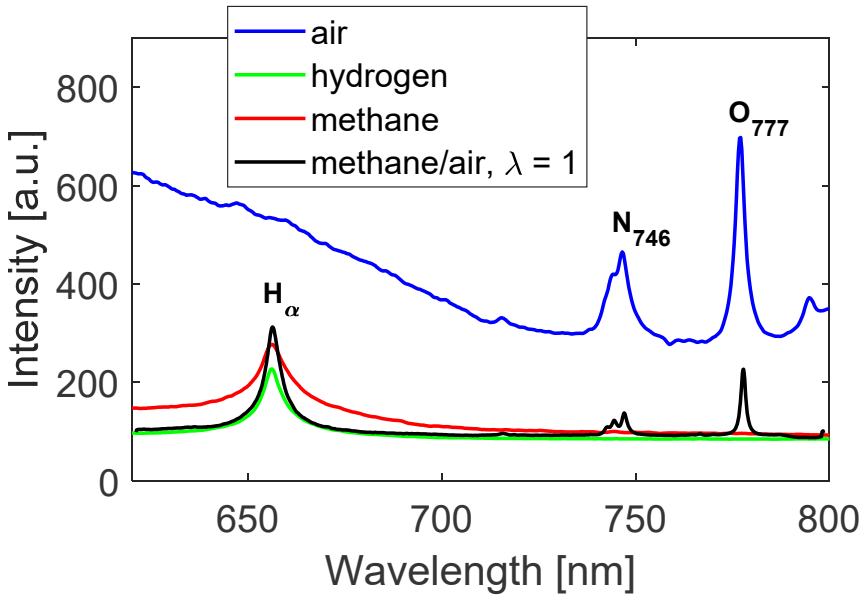

Figure 11: Spectral emissions for pure gases and for methane/air mixture, at exposure time t_e = 5 µs, absolute pressure 10 bar.

The correlation of spectral emissions features to the mixture air to fuel ratio was investigated for methane/air mixtures at different air to fuel ratios. Tests were performed at 10 bar absolute pressure, with 2 ms exposure time.
The molecular emission lines used are CN at 388 nm, OH at 306 nm and NH at 336 nm. Figure 12 shows the obtained spectra for air to fuel ratio (λ) ranging from 0.6 to 1.4. The corresponding molecular ratios (CN/NH and CN/OH) are plotted in Figure 13.

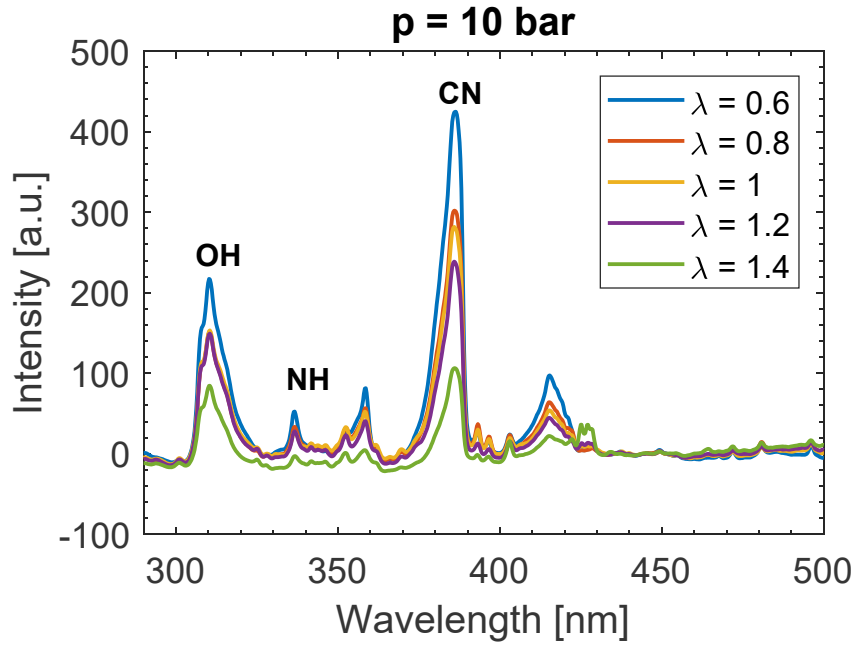

Figure 12: Spectral emissions for methane/air mixture for different air to fuel ratios. Exposure time: 2 ms.

Although a decreasing trend in molecular ratios towards lean mixtures is obtained, the shot to shot variations are high. This can be explained taking into account the long exposure time selected, which results in measurements' high sensitivity to phenomena such as re-strikes, re-attachments, plasma channel deflections.

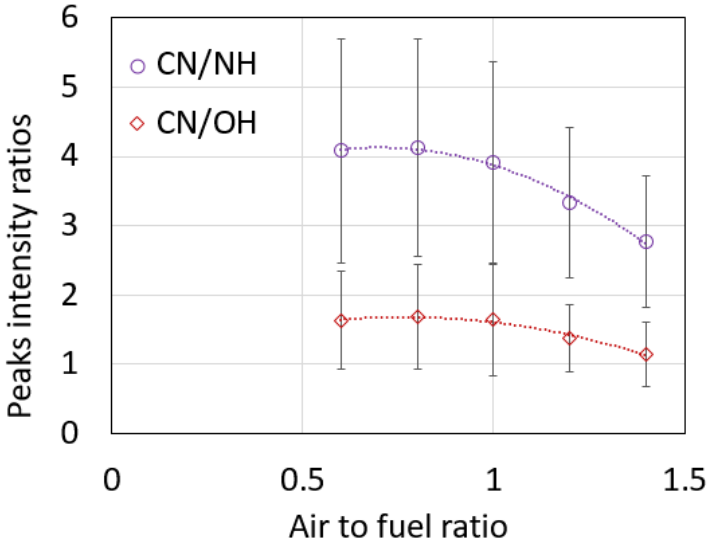

Figure 13: CN/NH and CN/OH intensity ratios at different air to fuel values.

In order to improve the standard deviation on the results, a similar investigation was performed taking into account atomic emissions. In this case, an exposure time of 5μs was used and the emission lines for H_α (656 nm), N (746 nm) and O (777 nm) were taken into account.
The emission spectra obtained, and the calculated trends for H/O and H/N ratios are shown in Figure 14 and Figure 15, respectively.

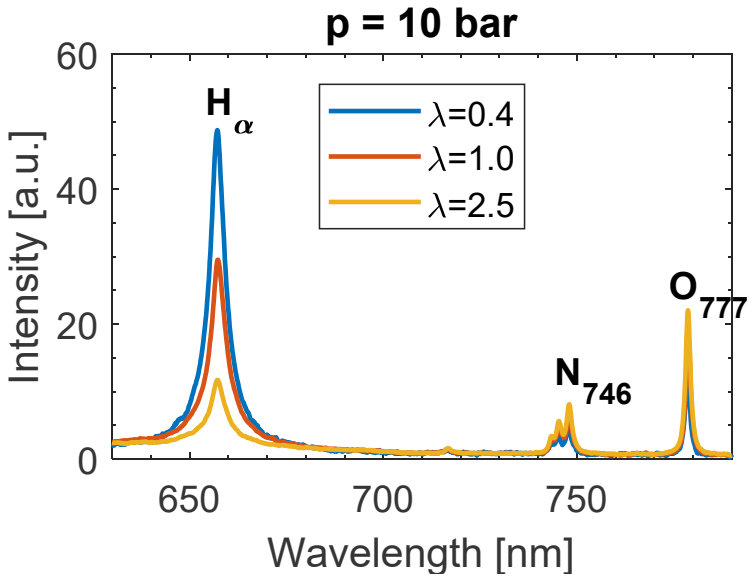

Figure 14: Spectral emissions for methane/air mixture for different air to fuel ratios. Exposure time: 5 μs.

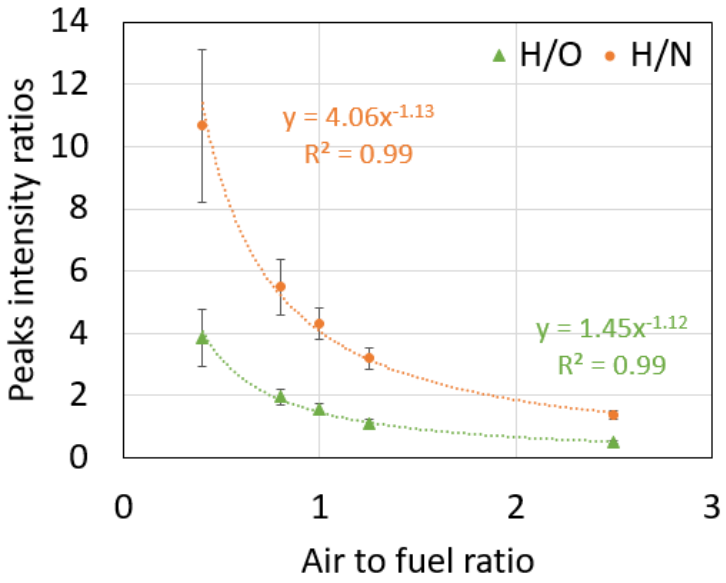

Figure 15: H/O and H/N intensity ratios at different air to fuel values.

In this case, a clearer trend is obtained, which allows correlating the air to fuel ratio with the peaks intensity ratios, and thus obtaining information on the local mixture concentration. The best signal to noise ratio is obtained for H/O ratio.

4. Conclusions and future work

A SIBS-based diagnostic technique for local air to fuel ratio investigation was successfully developed for ignition characterization in a small constant volume cell. Results are presented in this paper for different quiescent mixture compositions at ambient temperature and elevated pressure conditions. The role of methane, air and hydrogen on the electrical discharge characteristics and the plasma emissions are discussed. Moreover, spectral emissions in different ambient conditions and for different mixtures were compared and discussed, with the aim to obtain a deeper insight on the SIBS response to the complex physical and chemical phenomena underlying the ignition event. Emissions from single gases (pure air, methane, hydrogen and nitrogen) were measured at different exposure times, showing that atomic emission lines from oxygen, nitrogen and hydrogen can be recognized at shorter gating, while molecular emissions (C_2 and N_2) can be identified for longer exposure time. The role of delay time was also discussed, showing that atomic peaks in air at 10 bar can be recognized up to approximately 1 µs from breakdown. Peak intensity ratios of di-atomic carbon with the hydrogen Balmer-α was measured in methane-hydrogen mixtures with hydrogen volumetric content ranging from 0 to 100%, showing a matching trend with the hydrogen mass fraction in the mixture. Finally, reactive methane/air mixtures were investigated both in terms of molecular and atomic emissions vs. air to fuel ratio. Results show that a lower shot to shot variation and a clearer trend with mixture composition is found when atomic lines are used, with best signal to noise ratios for H/O ratios.

The results reported in this paper show that the proposed technique is a compact and versatile tool for applications involving atomic and molecular species detection in different ambient conditions.
In order to apply the SIBS-based diagnostic tool to running engines, further development is needed. For this purpose, a modified spark plug with fiber optics was designed and implemented with the aim to transfer the SIBS diagnostic technique from the constant volume cell to engine test rigs. Work is ongoing to test the feasibility of the fiber-optics equipped spark plug for SIBS diagnostics in the setup described in this paper, and subsequently in running engines.

Acknowledgements

This study was conducted within the RENERG2-project of the Swiss Competence Center of Energy and Mobility and financially supported by the Swiss Federal Office of Energy (SFOE, grant no. SI/500910-01), Volkswagen Corporate Research and the Research, Development and Promotion Foundation of the Swiss Gas Industry.

References

[1] U. Spicher, T. Heidenreich, Stratified-charge combustion in direct injection gasoline engines, in: Adv. Direct Inject. Combust. Engine Technol. Dev., Elsevier, 2010: pp. 20–44. doi:10.1533/9781845697327.20.
[2] Aleiferis PG, Taylor AMKP, Ishii K, Urata Y, The nature of early flame development in a lean-burn stratified-charge spark-ignition engine, Combust. Flame. 136 (2004) 283–302. doi:10.1016/j.combustflame.2003.08.011.
[3] Y. Takagi, A new era in spark-ignition engines featuring high-pressure direct injection, Symp. Int. Combust. 27 (1998) 2055–2068. doi:10.1016/S0082-0784(98)80052-0.
[4] P. Danaiah, R. Kumar P, V. Kumar D., Lean Combustion Technology for Internal Combustion Engines: a Review, Sci. Technol. 2 (2012) 47–50. doi:10.5923/j.scit.20120201.09.
[5] J.H. Weaving, Stratified Charge Engines, in: J.H. Weaving (Ed.), Intern. Combust. Eng. Sci. Technol., Springer Netherlands, Dordrecht, 1990: pp. 137–171. doi:10.1007/978-94-009-0749-2_5.
[6] T.D. Fansler, D.L. Reuss, V. Sick, R.N. Dahms, Invited Review: Combustion instability in spray-guided stratified-charge engines: A review, Int. J. Engine Res. 16 (2015) 260–305. doi:10.1177/1468087414565675.
[7] R.M. Merer, J.S. Wallace, Spark spectroscopy for spark ignition engine diagnostics, SAE Tech. Pap. (1995). doi:10.4271/950164.
[8] R. Maly, Spark ignition: its physics and effect on the internal combustion engine, in: Fuel Econ., Springer, 1984: pp. 91–148.
[9] D.R. Ballal, A.H. Lefebvre, The influence of flow parameters on minimum ignition energy and quenching distance, Symp. Int. Combust. 15 (1975) 1473–1481. doi:10.1016/S0082-0784(75)80405-X.

[10] C.C.O.B. Reynolds, R.L. Evans, Improving emissions and performance characteristics of lean burn natural gas engines through partial stratification, Int. J. Engine Res. 5 (2004) 105–114. doi:10.1243/146808704772914282.
[11] H. Biffiger, P. Soltic, Effects of split port/direct injection of methane and hydrogen in a spark ignition engine, Int. J. Hydrog. Energy. 40 (2015) 1994–2003. doi:10.1016/j.ijhydene.2014.11.122.
[12] P. Soltic, T. Hilfiker, S. Hänggi, R. Hutter, M. Weissner, Ignition- and combustion concepts for lean operated passenger car natural gas engines, in: Sustain. Altern., FKFS, Stuttgart, 2017.
[13] W. Lee, J. Wu, Y. Lee, J. Sneddon, Recent Applications of Laser-Induced Breakdown Spectrometry: A Review of Material Approaches, Appl. Spectrosc. Rev. 39 (2004) 27–97. doi:10.1081/ASR-120028868.
[14] L. Merotto, M. Sirignano, M. Commodo, A. D'Anna, R. Dondè, S. De Iuliis, Experimental Characterization and Modeling for Equivalence Ratio Sensing in Non-premixed Flames Using Chemiluminescence and Laser-Induced Breakdown Spectroscopy Techniques, Energy Fuels. 31 (2017) 3227–3233. doi:10.1021/acs.energyfuels.6b03094.
[15] F. Ferioli, S.G. Buckley, Measurements of hydrocarbons using laser-induced breakdown spectroscopy, Combust. Flame. 144 (2006) 435–447. doi:10.1016/j.combustflame.2005.08.005.
[16] S. Joshi, D.B. Olsen, C. Dumitrescu, P.V. Puzinauskas, A.P. Yalin, Laser-induced breakdown spectroscopy for in-cylinder equivalence ratio measurements in laser-ignited natural gas engines, Appl. Spectrosc. 63 (2009) 549–554.
[17] T.X. Phuoc, F.P. White, Laser-induced spark for measurements of the fuel-to-air ratio of a combustible mixture, Fuel. 81 (2002) 1761–1765. doi:10.1016/S0016-2361(02)00105-9.
[18] K.M. Abdul Rahman, N. Kawahara, D. Matsunaga, E. Tomita, Y. Takagi, Y. Mihara, Local fuel concentration measurement through spark-induced breakdown spectroscopy in a direct-injection hydrogen spark-ignition engine, Int. J. Hydrog. Energy. 41 (2016) 14283–14292. doi:10.1016/j.ijhydene.2016.05.280.
[19] M.H. Morsy, Review and recent developments of laser ignition for internal combustion engines applications, Renew. Sustain. Energy Rev. 16 (2012) 4849–4875. doi:10.1016/j.rser.2012.04.038.
[20] N. Kawahara, E. Tomita, S. Takemoto, Y. Ikeda, Fuel concentration measurement of premixed mixture using spark-induced breakdown spectroscopy, Spectrochim. Acta Part B At. Spectrosc. 64 (2009) 1085–1092. doi:10.1016/j.sab.2009.07.016.
[21] T.D. Fansler, B. Stojkovic, M.C. Drake, M.E. Rosalik, Local fuel concentration measurements in internal combustion engines using spark-emission spectroscopy, Appl. Phys. B Lasers Opt. 75 (2002) 577–590. doi:10.1007/s00340-002-0954-0.
[22] N. Kawahara, S. Hashimoto, E. Tomita, Spark discharge ignition process in a spark-ignition engine using a time series of spectra measurements, Proc. Combust. Inst. 36 (2017) 3451–3458. doi:10.1016/j.proci.2016.08.029.
[23] K. Kuwahara, H. Ando, Diagnostics of in-cylinder flow, mixing and combustion in gasoline engines, Meas. Sci. Technol. 11 (2000) R95–R111. doi:10.1088/0957-0233/11/6/202.
[24] T. Kammermann, W. Kreutner, M. Trottmann, L. Merotto, P. Soltic, D. Bleiner, Spark-induced breakdown spectroscopy of methane/air and hydrogen-enriched methane/air mixtures at engine relevant conditions, Spectrochim. Acta Part B At. Spectrosc. 148 (2018) 152–164. doi:10.1016/j.sab.2018.06.013.